

Investigation of 2-electrons systems for interpreting local correlation mechanisms in ionic compounds

Sébastien RAGOT[#], Jean-Michel GILLET[#], Pierre J. BECKER^{#@}

[#] Laboratoire Structure, Propriété et Modélisation des Solides (CNRS, Unité Mixte de Recherche 85-80). École Centrale Paris, Grande Voie des Vignes, 92295 CHATENAY-MALABRY, FRANCE

[@] Université Catholique de l'ouest. 1, place André-Leroy. BP808, 49008 ANGERS Cedex 01, FRANCE

Abstract

Electron correlation effects are often invoked as possible candidates to explain differences observed between experimental and Hartree-Fock (HF) Compton profiles. The shape as well as the magnitude of these differences can be very different, depending on the systems investigated. In order to illustrate this, simple analytical wave functions (WFs) for 2-electrons systems are proposed, which are correlated through radial and/or angular correlation factors. The “near-exact” densities obtained give us the opportunity to illustrate the dilemma that occurs when modeling momentum densities from Kohn-Sham (KS) orbitals. *Ab initio* studies follow for the analysis of correlation mechanisms in isolated ionic systems. opposite trends observed for experimental deviations to HF Compton profiles are then qualitatively explained through empirical models.

Keywords: 2-electrons systems, radial correlation, angular correlation, momentum space, Kohn-Sham orbitals.

I. Introduction

X-rays scattering experiments often reveal systematic deviations to HF calculations of impulse Compton profiles¹. Let denote by $\Delta J_{Exp}(q, \mathbf{u})$ the experimental deviation to the HF profile, *i.e.* $\Delta J_{Exp}(q, \mathbf{u}) = J_{Exp}(q, \mathbf{u}) - J_{HF}(q, \mathbf{u})$, where q stands for the momentum variable and \mathbf{u} is the direction of observation. In the case of cubic ionic crystals, the difference $\Delta J_{Exp}(q, \mathbf{u})$ is mainly isotropic², so that dependence on \mathbf{u} can be dropped in first approximation: $\Delta J_{Exp}(q, \mathbf{u}) \approx \Delta J_{Exp}(q)$. The experimental deviation $\Delta J_{Exp}(q)$ might further show opposite trends, depending on materials studied. For example, it is observed $\Delta J_{Exp}(0) < 0$ in the case of LiH and $\Delta J_{Exp}(0) > 0$ for MgO². Among various experimental effects, correlation effects are often invoked to explain these discrepancies. How can the same physical effect explain two opposite trends for $\Delta J_{Exp}(q)$?

To answer this question, we first refined empirical correlation (*i.e.* correlated – HF) Compton profiles straightforwardly on ΔJ_{Exp} . Despite a nice agreement, refined parameters do not permit to get a clear picture of mechanisms involved² and can further be misleading, since other experimental effects occur¹⁻³. We have therefore recently performed *ab initio* calculations³ on clusters, which accredited the possibility for correlation as responsible for both opposite effects. Meanwhile, we try to propose a simple model to interpret correlation mechanisms in momentum space. To this aim, we cast intra-atomic correlation into two mechanisms, *i.e.* angular and radial correlation effects. These effects have been widely studied and explained in terms of contributions to the correlation energy (see for example reference 19 and references therein). However, only few studies (like that of Meyer, Müller and Schweig⁴) do report analyses of correlation effects on observable quantities. All the more, possible consequences of different correlation mechanisms have never been analyzed, to our

knowledge, for the interpretation of opposite trends observed for the experimental deviation ΔJ_{Exp} .

We first compare angularly versus radially correlated distributions (section II) of some 2-electrons systems. Since correlated charge densities approach exact ones, we can analyze “near-exact” KS orbitals in momentum space (section III). Configuration interaction (CI) calculations on isolated ions then confirm that correlation in valence shells leads to the most visible part of deformations (section IV). They further accredit the assumption of correlation as responsible for the observed deviation to HF profiles. Finally, an empirical model where anions are artificially confined near the nucleus suggests that an enhanced angular correlation mechanism (section V) might be responsible for the trend observed for LiH correlation profiles.

II. 2-electrons systems : radial versus angular correlation mechanisms

The helium problem became a whole challenge already at the early days of the quantum theory: scientists were trying to convince of the pertinence of Schrödinger equation for studying atomic systems. In 1928, Hylleraas⁵ determined a WF so accurate that his method inspired many other studies like James and Coolidge’s one for H_2 ⁶. The same year, Slater⁷ analyzed the correlated hamiltonian $H = h_1 + h_2 + 1/r_{12}$ and shown that the divergence at the coalescence point ($r_{12} = 0$) brings a cusp in the exact WF, which must in turn exhibit a linear r_{12} dependence near $r_{12} = 0$. It is well known since Hylleraas work that introducing the variable r_{12} in the WF ensures a fast convergence of the correlation energy. Following this idea, a formidable number of accurate analytical WFs have been then suggested so that is rather challenging to report all the corresponding studies. The reader interested may consult

references 8,9,10,11,12 and references therein. Note that Hylleraas-like WFs are still widely used^{13,14}, notably in the field of atomic physics.

Unfortunately, such functions become rapidly prohibitive as the number of electron increases. All the more, the analytical evaluation of the subsequent electron distributions in momentum space clearly makes the use of Hylleraas-like WFs a torment. The compromise adopted here bypasses this difficulty: it relies on a partial separation of angular and radial effects, as suggested when developing the term

$$\frac{1}{r_{12}} = \frac{1}{r_{>}} + \frac{r_{<}}{r_{>}} \cos \mathcal{G}_{12} + \dots \quad (1)$$

where $r_{>}$ denotes the sup of (r_1, r_2) . The whole potential can be thus developed as $v(r_1, r_2) \equiv v(r_{<}, r_{>}) = -Z/r_{>} - Z/r_{<} + 1/r_{>} + \dots$. This expression shows that the external part of the electronic cloud experiences a screening of the nucleus due to the internal part, which mechanism invokes *radial* correlation. In the case of a low nuclear charge ion (*i.e.* H⁺), the screening is proportionally more important. Following terms further imply *angular* correlation through the inter-particle angle \mathcal{G}_{12} .

In order to reflect both radial and angular effects while keeping a separable character, the trial WF chosen is

$$\Psi(\mathbf{r}_1, \mathbf{r}_2) = c_{\alpha\beta} \left(e^{-\alpha r_1 - \beta r_2} + e^{-\beta r_1 - \alpha r_2} \right) (1 - b_{\alpha\beta} \mathbf{r}_1 \cdot \mathbf{r}_2) \quad (2)$$

$$+ c_{\alpha} e^{-\alpha(\eta_1 + r_2)} (1 - b_{\alpha} \mathbf{r}_1 \cdot \mathbf{r}_2) + c_{\beta} e^{-\beta(\eta_1 + r_2)} (1 - b_{\beta} \mathbf{r}_1 \cdot \mathbf{r}_2)$$

The terms $e^{-\alpha r_1 - \beta r_2}$ and $(1 - b \mathbf{r}_1 \cdot \mathbf{r}_2)$ respectively simulate radial and angular correlation effects. We acknowledge that the definition of radial and angular correlation is rather vague, that is, terms like $(1 - b \mathbf{r}_1 \cdot \mathbf{r}_2)$ contain angular correlation through the term $\cos \mathcal{G}_{12}$ but not only. This approach is further *less efficient* than the Hylleraas-like. However, the lack of singularity at $r_{12} = 0$ greatly simplifies the analytical calculation of Compton profiles. The uncorrelated

HF reference WF is chosen as an optimized triple-zeta one, so that in the following, all say “correlation quantities” refer to the difference correlated – HF.

The trial WF (2) reveals all the more to be accurate for ions of lower nuclear charge (like H⁻), for which the mutual screening of electrons is proportionally more important. Values of correlation energies ε obtained are scheduled in table 1. The WF (2) can be reduced to a function mainly “angularly” correlated by imposing the constraints $C_{\alpha\beta} = \sqrt{C_\alpha C_\beta}$ and $b = b_\alpha = b_\beta = b_{\alpha\beta}$, *i.e.* it reduces to $(\sqrt{c_\alpha} e^{-\alpha r_1} + \sqrt{c_\beta} e^{-\beta r_1})(\sqrt{c_\alpha} e^{-\alpha r_2} + \sqrt{c_\beta} e^{-\beta r_2})(1 - b \mathbf{r}_1 \cdot \mathbf{r}_2)$. Conversely, angular correlation is switched off by putting $b_k = 0 \quad \forall k$ in (2). Resulting WFs are optimized separately, resulting in correlation energies, which are obviously not fully independent. In table 1, we observe that the energy of *radial* correlation is proportionally more important for the lower nuclear charge ion. Conversely, angular correlation energy seems to increase with Z (while $Z < 3$). For $Z > 2$, the model WF clearly becomes insufficient for describing the angular correlation due to the low angular expansion of the trial WF. Let us nevertheless point out that whereas exact correlation energies remain almost constant (table 1), the magnitudes of correlation densities drastically decrease as the nucleus charge increases (figure 1): this conclusion holds for ions of $Z > 2$. The correlation charge densities reported on are radial quantities (*i.e.* multiplied by $4\pi r^2$), which allows for an appreciation of correlation effects at large values of r . All curves integrate to zero, since they are defined as the difference between two normalized distributions. We have checked that variational densities compare well with *ab initio* ones, calculated in very extended basis sets: correlation densities of H⁻ obtained from the trial WF (2) revealed to be quasi-identical to those delivered by Gaussian94¹⁵ (CI – HF calculation within AUG-cc-pV5Z basis-set¹⁶).

We also compare angularly, radially and globally optimized correlation densities for H⁻ and He. Subsequent deformations are reported on figure 1 for the charge density (left column) and the Compton profiles (right column). Note that the magnitudes of the

deformations are very sharp in \mathbf{P} -space for the H^- diffuse ion. The larger magnitudes are associated to lower nuclear charge ions, which suggests the most visible correlation deformations shall more generally be associated to valence electrons. The possibility for angular correlation alone allows the electron cloud to get closer to the nucleus, while slightly shifting the Compton profile towards higher momenta. The subsequent *correlation* profile is thus negative at zero momentum ($\Delta J_{\text{Corr,Ang}}(0) < 0$), which feature is for instance observed in the case of LiH. Radial correlation alone widens the electron distributions. However, we can point out that deformations in \mathbf{P} -space are systematically positive at large q , consistently with the Virial theorem, which implies that correlation increases the kinetic energy. Besides, we observed in the case of H^- that correlation effects are more pronounced on Compton profiles than on form factors: maximum relative deviations being respectively of about 20% and 5% (not reported). The magnitudes of the deformations become however similar for neutral and positive species (<1%).

The observed deformations reflect the error associated with the mean field approximation: for instance, one can conclude that the HF approximation overestimates electron distributions near $\langle x \rangle$, where $x = r, q$. This interpretation, which is just so fine, holds for the momentum density of light 2-electrons systems but is not straightforwardly extensible to heavier ions.

III. Momentum space: KS, CI and others

Let us shortly deviate from our initial concern to examine KS orbital in momentum space. The momentum density is defined as $n(\mathbf{p}) = \frac{1}{(2\pi)^3} \int \rho_1(\mathbf{r}, \mathbf{r}') e^{i\mathbf{p} \cdot (\mathbf{r} - \mathbf{r}')} d\mathbf{r} d\mathbf{r}'$, implying thereby ρ_1 , the exact 1-electron reduced density matrix integrated over spin variables (1RDM) or at least an N -representable one. The momentum density can subsequently not be straightforwardly derived from a KS determinant, except for practical reasons. Rather, it

should be defined as a functional of the density, like any other electronic property. It is therefore interesting to understand the error inherent to momentum distributions obtained from KS orbitals, *i.e.* in the framework of density functional theory (DFT). As pointed out by Savin during a recent intimate workshop¹⁷: it is necessary to distinguish between the “true” DFT from the “zoology” inherent to the choice of appropriate functionals before concluding on the potential of DFT for momentum space.

Therefore, we take advantage of dealing with 2-electrons systems to define the unique KS orbital as $\varphi_{KS}(\mathbf{r}) = \sqrt{\rho(\mathbf{r})/2}$, in the same way than Qian and Sahni did while analyzing properties of the Hooke’s atom¹⁸. Considering the reference correlated density $\rho(\mathbf{r})$ obtained from (2) as the exact one, we calculate numerically the Fourier transform of the KS orbital (χ_{KS}), from which is obtained the KS momentum density: $n_{KS}(\mathbf{p}) = 2|\chi_{KS}(\mathbf{p})|^2$. The correlated, HF and KS radial momentum densities of H⁻ are compared on figure 2. It is striking that $n_{KS}(\mathbf{p})$ is closer to $n(\mathbf{p})$ than $n_{HF}(\mathbf{p})$. The same observation holds for He (not reported). We are then tempted to conclude that KS orbitals may lead to more accurate momentum densities than HF ones, *i.e.* that KS orbitals contain part of the correlation effects. However, the corresponding increase of the kinetic energy is only 0.008 u.a. (KS – HF), which must be compared to the exact (0.039 u.a.) or the present one (0.035 u.a. from WF 2–HF), revealing thereby a lack of correlation-induced momentum transfer. Indeed, while 1RDMs derived from single determinants write as a finite sum of orbital products (only 1 in the present case), exact 1RDMs require a sum of infinite terms, revealing strong connections between \mathbf{r} and \mathbf{r}' variables.

This point can be easily understood through a simple example: the harmonium atom. The harmonium atom is a fictive system of 2 fermions trapped in a harmonic potential while repelling each other through the Hooke’s law. This system has been proposed by Davidson¹⁹ and later reused by Thakkar²⁰ in order to illustrate correspondences between the various

electron distributions. Such a system is exactly solvable, which allows us to compare exact, HF and KS density matrices, respectively denoted by $\rho_{1,Exact}$, $\rho_{1,HF}$ and $\rho_{1,KS}$. Expressions obtained for the 1-matrices are

$$\rho_{1,Exact}(\mathbf{r}, \mathbf{r}') \propto e^{-\alpha(\mathbf{r}'+\mathbf{r})^2/4 - \beta(\mathbf{r}'-\mathbf{r})^2/4}$$

$$\rho_{1,HF}(\mathbf{r}, \mathbf{r}') \propto e^{-\gamma(\mathbf{r}^2+\mathbf{r}'^2)/2}$$

$$\rho_{1,KS}(\mathbf{r}, \mathbf{r}') \propto e^{-\alpha(\mathbf{r}^2+\mathbf{r}'^2)}$$

where α , β , and γ are some positive constants. Since $\alpha \neq \beta$, the exponent in $\rho_{1,Exact}$ is not proportional to $\mathbf{r}^2 + \mathbf{r}'^2$; $\rho_{1,Exact}$ can therefore not be rewritten as a gaussian orbital product whereas $\rho_{1,HF}$ and $\rho_{1,KS}$ can. In other word: fermion repulsion does not only correlate one particle with an other one but it also correlates one particle with itself (through the difference $\mathbf{r}'-\mathbf{r}$).

Besides, we have checked that *ab initio* calculations resulted in more accurate KS than HF momentum densities in the case of H^- , whereas the KS momentum density obtained for He revealed much less accurate than the HF one (using Becke's 88 functional for exchange²¹ and Perdew/Wang's 91 correlation functional²²). This obviously recommends being cautious while interpreting KS orbitals in momentum space, especially when looking at correlation effects.

IV. Valence versus global correlation effects in isolated ionic systems

As suggested from the previous section, it is more convenient to deal with explicitly correlated WFs for momentum space considerations. However, an accurate *ab initio* determination of a property $\Delta f(\mathbf{x}) = f_{CI}(\mathbf{x}) - f_{HF}(\mathbf{x})$ requires very extended basis-sets (BSs), which make the calculations rarely feasible. Quantities in momentum space are indeed very

sensitive to the choice of the BS⁴; we observed that magnitudes of correlation densities estimated from cc-pVTZ and cc-pV6Z basis sets¹⁶ can vary of a factor 3 in the case of light ions. We report correlation effects on radial densities on figure 3 and 4 (\mathbf{R} and \mathbf{P} -space, respectively) for a closed-shell negative ion (F^-). The calculation was performed at CISD/cc-pV5Z level¹⁶: CISD stands for CI with all single and double excitations. This was achieved by interpreting in momentum space the 1RDM: $\rho_1(\mathbf{r}, \mathbf{r}') = \sum_{i,j} c_{ij} \varphi_i(\mathbf{r}) \varphi_j(\mathbf{r}')$, as obtained from a Gaussian94 calculation. The products $\varphi_i \varphi_j$ were further cast into core-core (c - c), core-valence (c - v) and valence-valence (v - v) contributions. The 1RDM finally decomposes as $\rho_1 = \rho_1^{cc} + \rho_1^{cv} + \rho_1^{vv}$: each resulting contribution is shown on figure 3 and 4 (in both \mathbf{R} and \mathbf{P} -space, respectively). As suggested from 2-electrons calculations, almost all the visible deformations arise due to valence electrons. It thus allows for modeling correlation effects in valence shells only in first approximation. The observed deformations are further qualitatively similar to that of 2- or 10-electron systems and contribute up to 2.6% of the global MD but this value is probably widely underestimated (they indeed reach 18% in the case of H^-), due to the limited basis-set we used.

The comparison of correlation momentum densities of He, Ne and F^- , calculated at CISD/cc-pV5Z level, has shown that correlation effects increase with both the number of electrons and the level of ionicity (not reported). This suggests that ionic crystals be potential candidates for the observation of electron correlation effects in \mathbf{P} -space. Besides, we have noticed that the shapes of correlation profiles of 2 and 10-electron systems exhibit some qualitative resemblance with that both theoretically and experimentally observed for MgO crystals^{2,3}.

Conversely, correlation in 4-electron systems yields much larger magnitudes for the correlation-induced deformations⁴, together with the property $\Delta J_{\text{Corr}}(0) < 0$. For such systems, the usual proximity of the levels $2s/2p$ enhances the angular correlation character.

V. Interpretation of opposite trends obtained for experimental deviations to Compton profiles of some ionic compounds

We have recently shown that a cluster-based calculation, followed by an appropriate pseudo-atomic partition of the 1RDM (cluster partitioning method or CPM), enables an accurate evaluation of observable quantities^{3,23}. The method has been tested for generic materials like insulators (LiH, MgO), a semiconductor (Si) and a simple molecular crystal (Ice I_h). The main point is that the method is transparent in both \mathbf{R} and \mathbf{P} -spaces, which allows for a comparison between experimental and theoretical electron distributions in both spaces simultaneously. Restricting calculations to small clusters further allowed for a fair description of local correlation effects in ionic compounds on both Compton profiles and structure factors. In each case, correlation effects are mainly associated to the anions. Subsequent correlation profiles show a qualitative agreement with the observed experimental trends, that is, $\Delta J_{Corr}(0) < 0$ for LiH and $\Delta J_{Corr}(0) > 0$ for MgO.

So far, so good, but we did not get a clear picture of mechanisms involved. Therefore, assuming that mainly local correlation mechanisms are involved, we propose a simple 2-electrons model where both *angular* and *radial* correlation mechanisms compete. The nuclear charge of the ionic system is $Z = 1$. We make use of the former trial WF (2), while the uncorrelated reference wave function remains the triple-zeta one. The difference with isolated systems studied in section II is that electrons now experience an effective central potential which writes as $v_{eff} = -(1/r_1 + 1/r_2) + k(r_1^2 + r_2^2)$. The term $k(r_1^2 + r_2^2)$ is added to simulate the Pauli repulsion of surrounding pair of valence electrons and, in turn, confines electrons more or less close to the nucleus. Optimizing both correlated and uncorrelated wave functions enables an analytical evaluation of the correlation Compton profile, as reported on figure 5 for various values of k (respectively $k = 0.001, 0.005$ and 0.010 a.u.). Increasing ion confinement in crystal affects the trend of correlation profiles, notably near $q = 0$, *i.e.* it reduces the radial

correlation mechanism. The case $k = 0.010$ a.u. renders a correlation profile very close to that obtained from an *ab initio* calculation on a Li_1H_6 cluster (QCISD – HF calculation in an extended BS³), after averaging the periphery anion contributions. The Li_1H_6 cluster was embedded in a Madelung field for ensuring electrical neutrality. The two former curves are further in qualitative agreement with the experimental deviation observed for LiH (with the correct limit $\Delta J_{\text{Corr}}(0) < 0$), regardless of the magnitudes. These observations accredit the assumption of a preferred angular correlation mechanism for LiH. Since angular correlation enables electrons to get closer to the anionic nucleus, it reduces the size of the anion, which is consistent with the often-mentioned HF overestimation of anionic radii in LiH^{24} . On the other hand, smaller values of k render model correlation profiles resembling these of free 2- or 10-electrons systems, as well as this obtained from a cluster calculation on MgO^3 . We thus conclude that opposite trends observed for experimental deviations to HF Compton profiles of ionic compounds can result from different strengths of confinement of the embedded anion.

The theoretical correlation profile of LiH has a much lower magnitude than the experimental deviation, which must necessary have consequences on kinetic energies. Note that the transfer of one electron from Li to H forms a paired couple, the correlation energy of which wholly participate to the cohesion mechanism. The experimental cohesion energy was estimated²⁵ to 0.18 a.u. vs. 0.13 a.u. from HF calculation. The difference, 0.05 a.u., is close to the usually expected correlation energy for an isolated single pair¹⁹ (≈ -0.04 a.u.). For instance, the increase of kinetic energies due to correlation and involving the anion alone (Mulliken approximation) was estimated to 0.04 a.u. from the Li_1H_6 calculation, after averaging anionic kinetic energies. This value is consistent with the expected one (which should not exceed 0.05 a.u., through the Virial theorem), while the experimental deviation widely overestimates the correlation kinetic energy³.

Conversely, LiH crystal might be seen as an assembly of Li^- anions stabilized by an octahedral cage of protons. As already mentioned, correlation effects are well pronounced for 4-electron systems and yields large magnitude for correlation densities; they further deliver shapes of correlation profiles similar to that observed for LiH (with the property $\Delta J_{\text{Corr}}(0) < 0$, see reference 4).

VI. Conclusion

Simple analytical WFs allow for an analytic evaluation of correlation effects on observable quantities for 2-electrons systems. The choice we made that consists of a separation, in a certain extent, of radial and angular effects enables to illustrate the evolution of correlation mechanisms when the nuclear charge increases. Radial correlation mechanism is preponderant for low Z ions. The error inherent to mean field approximations is further characterized in a very simple manner in both spaces simultaneously. Two-electron correlation effects on momentum densities can be further partly recovered by using near-exact KS orbitals. The KS momentum density does otherwise not systematically improve the HF one when using standard functionals. *Ab initio* calculations confirm that mainly valence-shells correlation appreciably affects the 1-electron distributions, which allows for modeling correlation effects in the valence shell only as a first approximation. Therefore, we modeled anions in crystals like an effective 2-electrons system experiencing a confinement potential, which mimics the Pauli repulsion of surrounding paired electrons. The resulting correlation profile obtained is in very close agreement with previous results obtained from *ab initio* calculations performed on small cluster³. We concluded that opposite trends observed for experimental deviations to HF Compton profiles of ionic crystals can be interpreted as resulting from different strengths of confinement of the embedded anion.

TABLE CAPTION & TABLE

Table 1: Comparison of angular, radial and total correlation energies (from WF 2) of 2-electrons ions, expressed as a percent of the benchmark values of Davidson and Chakravorty²⁶

Table 1

	% ε (Ang)	% ε (Rad)	% ε (Tot)	ε exact
H ⁻	42%	64%	93%	-0.0395
He	49%	36%	84%	-0.0420
Li ⁺	49%	32%	81%	-0.0435
Be ²⁺	41%	29%	74%	-0.0443

FIGURE CAPTIONS & FIGURES

Figure 1: Comparison of correlation densities of some 2-electrons ions ($Z = 1$ and 2 : rows 1 to 2). *Left*: correlation effects on radial charge densities. *Right*: correlation effects on Compton profiles. *Full line*: from optimized WF (2). *Dashed*: from radially correlated WF. *Grey*: from angularly correlated WF. *Vertical dashed line*: position of $\langle x \rangle$, $x = r, q$.

Figure 2: Comparison of radial momentum densities of H⁻. *Full line*: from WF (2). *Small dashed*: from KS orbitals. *Large dashed*: from HF orbitals.

Figure 3: Radial electron densities of F⁻ in **R**-space. *Left*: CI distributions. *Right*: CI-HF distributions. *Full lines*: all electrons. *Dotted*: core-core contributions. *Dashed*: core-valence. *Dotted-dashed*: valence-valence

Figure 4: Radial electron densities of F⁻ in **P**- space. *Left*: CI distributions. *Right*: CI-HF distributions. *Full lines*: all electrons. *Dotted*: core-core contributions. *Dashed*: core-valence. *Dotted-dashed*: valence-valence.

Figure 5: Correlation Compton profiles of confined 2-electrons system. *Dotted line*: $k = 0.001$ a.u., *Dashed*: $k = 0.005$ a.u. *Full*: $k = 0.010$ a.u. *Thick dotted dashed*: correlation profiles calculated from a Li₁H₆ cluster, after averaging the periphery anion contributions. *Dots* (with statistical error bars): $\Delta J_{\text{Exp}} = J_{\text{Exp}} - J_{\text{Crystal95/HF}}$, from [27] and scaled by a 0.525 factor in order to match the residual deviation magnitude found by Bellaiche and Lévy²⁸ after correction for both impulse approximation and multiple scattering.

Figure 1

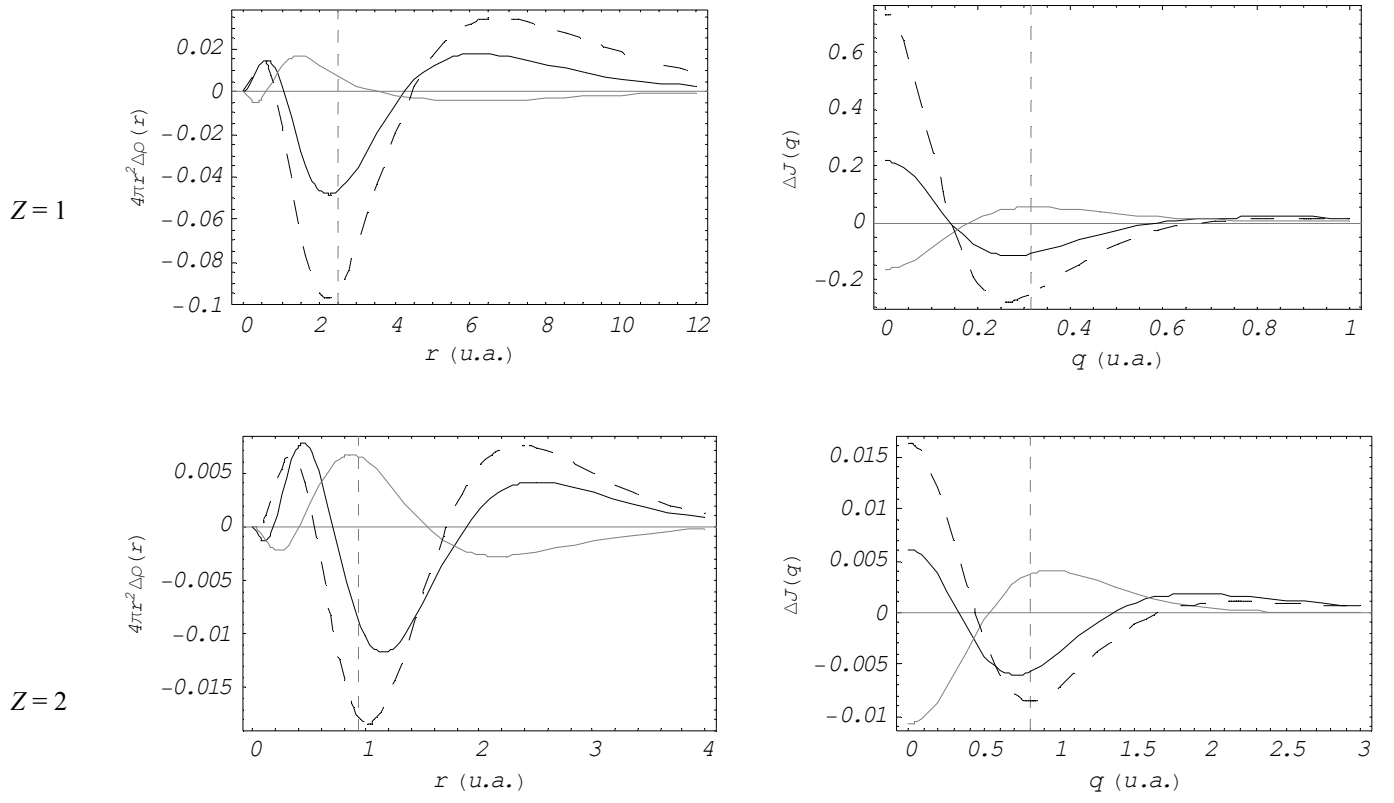


Figure 2

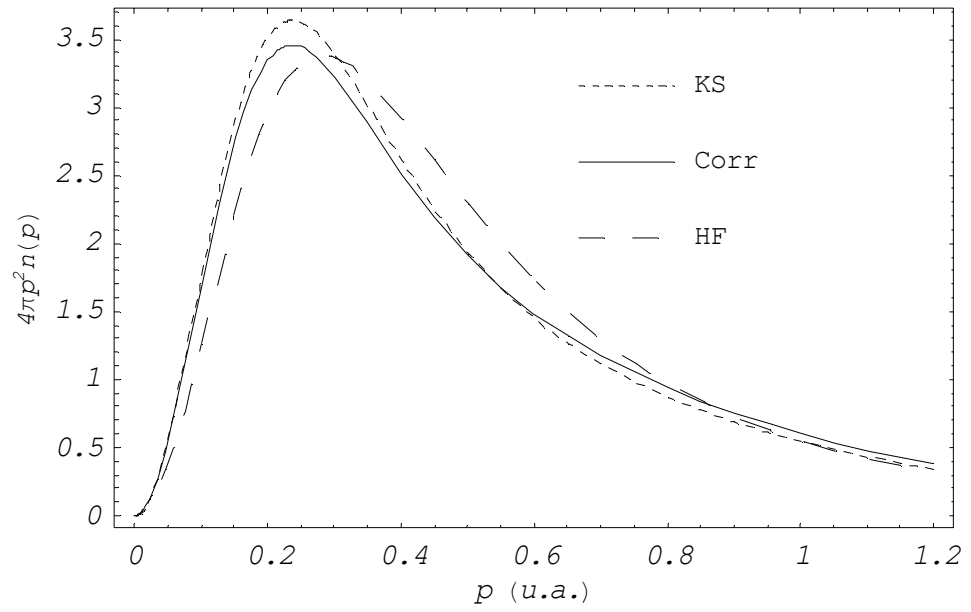


Figure 3

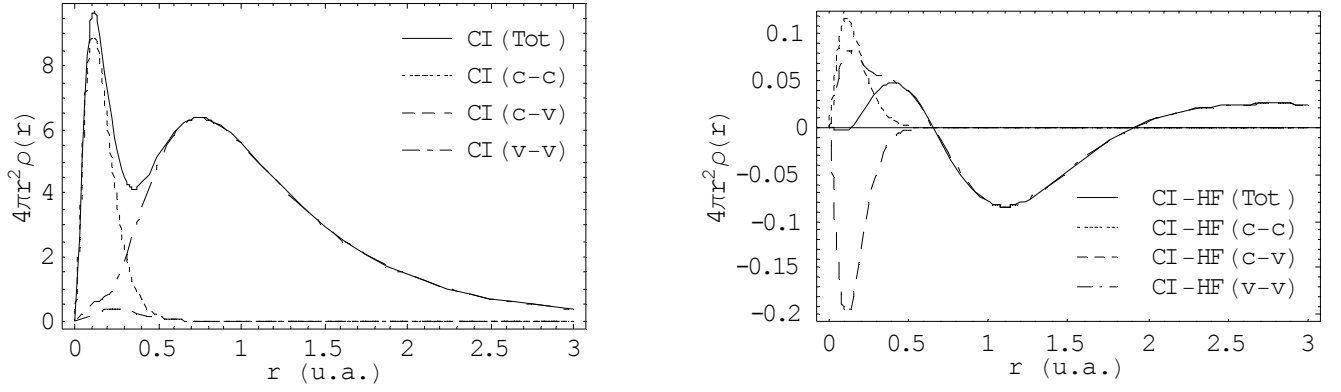


Figure 4

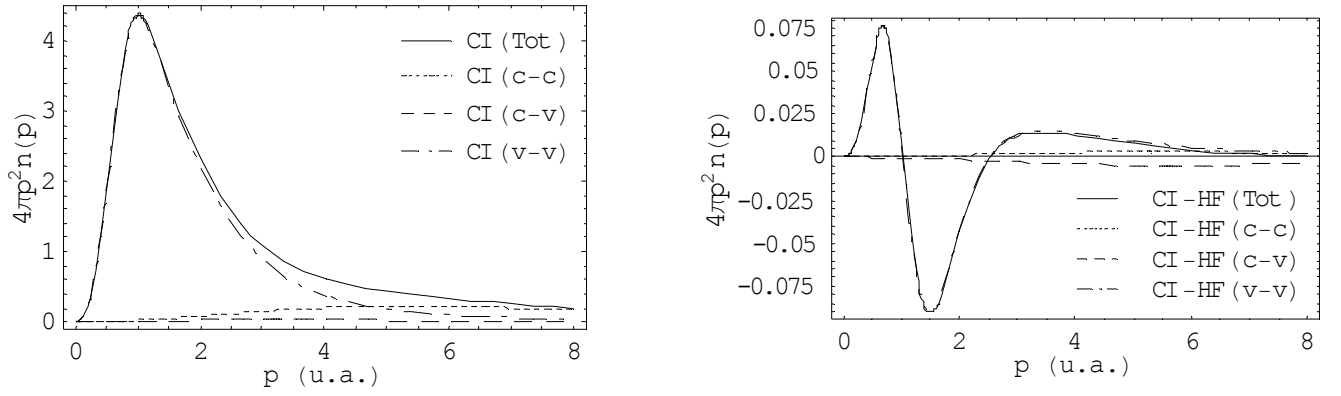
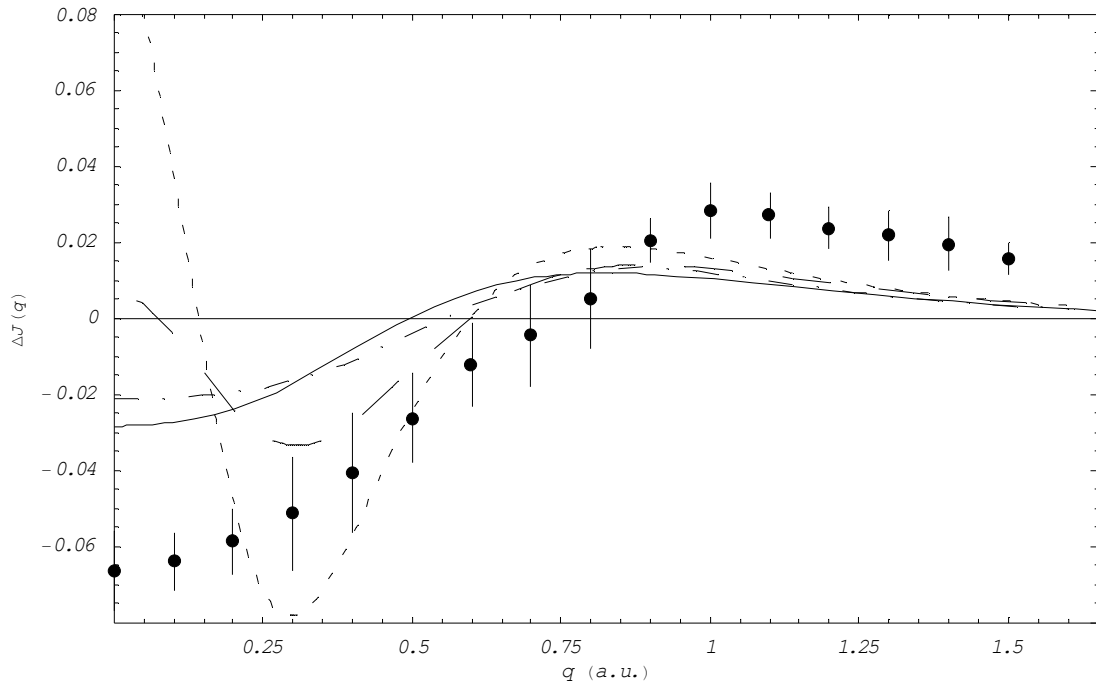


Figure 5



References

- ¹ Williams B. *Compton Scattering*. (1977) Mac-Graw Hill Inc.
- ² Becker P.J., Gillet J.M., Cortona P., Ragot S. TCA **105** (2001) 284
- ³ Ragot S., Gillet J.M., Becker P.J.: “*A cluster partitioning method: determination of density matrices of solids and comparison with X-ray experiments*”. Submitted to Phys. Rev. B
- ⁴ Meyer H. Müller T., Schweig A. J. Mol. Struct. (*Theochem*) **360** (1996) 55
- ⁵ Hylleraas E. A.: Z. Physik **48**, 469 (1928)
- ⁶ James H. M. and Coolidge A. S. J. Chem. Phys. **1** :825 (1933), Phys. Rev., **43** : 488 (1933), J. Chem. Phys., **3** :129 (1935)
- ⁷ Slater J. C. Phys. Rev. **31**, 333 (1928)
- ⁸ Hartree D. R., Ingman A. L 1933 Mem. Proc. Manchester Lit. Phil. Soc. **77** 79
- ⁹ Hartree D. R. 1957 *The Calculation of Atomic Structures* (New York: Wiley)
- ¹⁰ Tripathy D.N., Padhy B. and Rai D.K. J. Phys. B: At. Mol. Opt. Phys. **28** (1995) L41
- ¹¹ Bhattacharyya S., Bhattacharyya A., Talukdar B. and Deb N.C. J. Phys. B: At. Mol. Opt. Phys. **29** (1996) L147
- ¹² Le Sech C.. J. Phys. B: At. Mol. Opt. Phys. **30** (1997) L47
- ¹³ Moiseyev N. and Cederbaum L.S. J. Phys. B: At. Mol. Opt. Phys. **32** No 12 (1999)
- ¹⁴ Yan Z-C., Babb J.F., Dalgarno A., Drake G. W. F. Phys. Rev. A. **54** (1996) 2824
- ¹⁵ Gaussian 94, Revision D.4, Frisch M. J., Trucks G. W., Schlegel H. B., Gill P. M. W., Johnson B. G., Robb M. A., Cheeseman J. R., Keith T., Petersson G. A., Montgomery J. A., Raghavachari K., Al-Laham M. A., Zakrzewski V. G., Ortiz J. V., Foresman J. B., Cioslowski J., Stefanov B. B., Nanayakkara A., Challacombe M., Peng C. Y., Ayala P. Y., Chen W., Wong M. W., Andres J. L., Replogle E. S., Gomperts R., Martin R. L., Fox D. J., Binkley J. S., Defrees D. J., Baker J., Stewart J. P., Head-Gordon M., Gonzalez C., and Pople J. A., Gaussian, Inc., Pittsburgh PA, 1995
- ¹⁶ See reference above for information about available basis-sets or the Extensible Computational Chemistry Environment Basis Set Database (Web site: <http://www.emsl.pnl.gov:2080/forms/basisform.html>)
- ¹⁷ *Workshop on electron distributions* (24/04/01). Ecole Centrale Paris, France
- ¹⁸ Qian Z. and Sahni V. Phys. Rev. A. **57** (1998) 2527
- ¹⁹ Davidson E.R. “*Reduced Density Matrices in Quantum Chemistry*”, Academic Press, 1976
- ²⁰ Thakkar A. J. *et al.*: «*On one-Matrices and related densities*». *Density Matrices and Density Functionals*, eds., Erdahl R. M. and Smith V., Jr., 5-20, (1987) Riedel
- ²¹ Becke A.D. Phys. Rev. A. **38** (1988) 3098
- ²² Perdew J.P. and Wang Y. Phys. Rev. B. **45** (1992) 13244
- ²³ Ragot S., Gillet J.M., Becker P.J.: “*Interpreting Compton anisotropy of ice I_h : a cluster partitioning method*”. Submitted to Phys. Rev. B (2001)
- ²⁴ Shukla A., Dolg M., Fulde P., Stoll H. Phys. Rev. B **60** (1999) 5211
- ²⁵ See Anderson O.L., J. Phys. Chem. Solids. **27** (1966) 547 and ref. 24
- ²⁶ Davidson E.R. and Chakravorty S.J. J. Phys. Chem. 1996, 100, 6167
- ²⁷ Gillet J.M., Becker P., Loupiau G. (1995), *Acta Cryst. A*, **51** 405
- ²⁸ See Bellaïche L. and Lévy B. Phys. Rev. B **54** (1996) 1575